1 Part description

The chosen part is an idealized form of an aircraft spar – the flanges and web are modeled together as an I beam (as seen in Fig 1.1). It is assumed that this behaves as a cantilever beam, fixed at the wing root (connection to fuselage). The main aerodynamic loads on an aircraft wing are Lift (spanwise bending, supported by the spar) and Torsion loads (resisted by 'torsion box' – multiple spar and skin assembly). For sake of simplification, it is assumed that the predominant loading on a wing spar is bending, and the spar acts as a classical shear beam, with the flanges carrying compression/tension, and the web carrying shear loads.

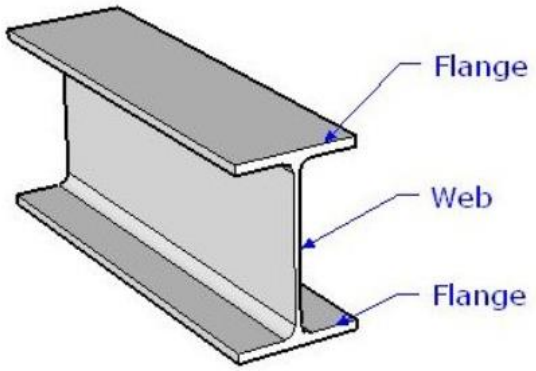

Figure 1.1: Spar idealized as an I-beam

Figure 1.2: Wing bending loads

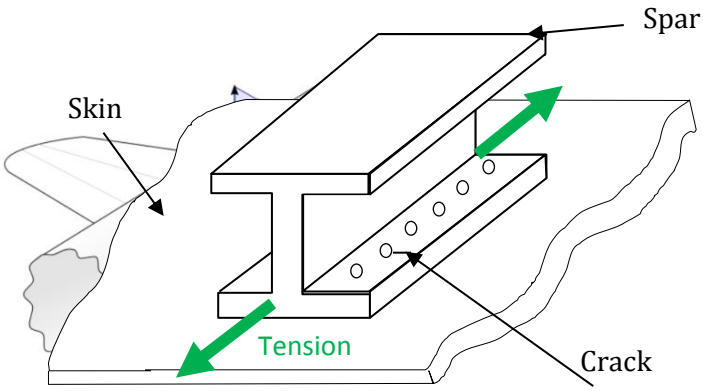

Figure 1.3: Loads on lower spar cap

The idealized lift distribution over a wing is seen in Fig 1.2. If a section of the span is considered for this analysis, we will look at the lower flange, which will be in tension. A crack is assumed to have initiated at a fastener location common to the spar flange and lower wing skin, as seen in Fig 1.3.

2 Stress Intensity

The geometry of the idealized I beam is given in Fig 2.1. For this analysis, only the effective width of the flange is considered for fatigue and crack growth – the radius/curved boundary effects are not considered, making this a conservative approach. The fastener at the joint is a HL10VAZ-8 (Titanium Shear), with a shear capability of 4,650lbs. The stress intensity factor is calculated for the scenario in Fig 2.3.

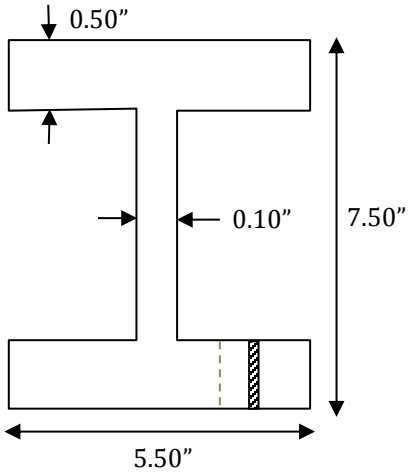

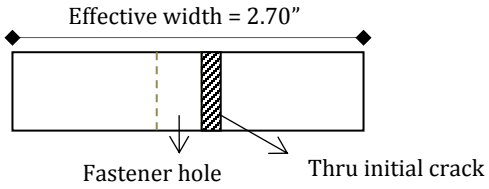

(Left) Figure 2.1: Spar Geometry

(Above) Figure 2.2: Flange modeled as a finite width plate

For symmetric cracks under uniform applied stress,

$\beta = \beta_1 + \beta_2$

$\beta_1 = F_{C/R} F_W F_{WW}$

$\beta_2 = (\sigma_{br}/\sigma) F_3 F_W F_{WW}$

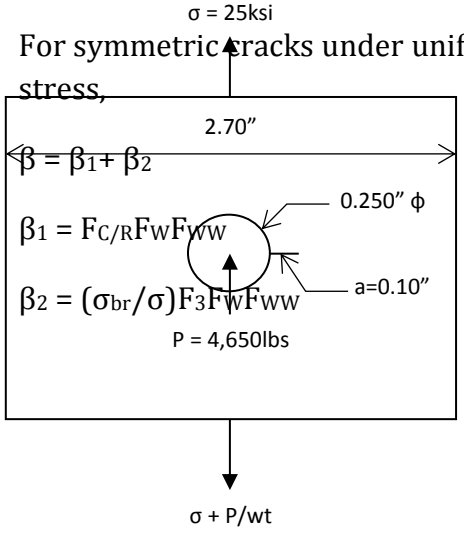

Figure 2.3: Crack growth at fastener location

$$F_{C/R} = \frac{3.404 + 3.1872\frac{C}{R}}{1 + 3.9273\frac{C}{R} - 0.00695\left(\frac{C}{R}\right)^2}$$

$$F_W = \sqrt{sec\frac{\pi R}{W} sec\frac{\pi(R+c)}{W}}$$

$$F_{WW} = 1 - \left(\left(1.32\frac{W}{D} - 0.14 \right)^{-\left(.98 + \left(0.1\frac{W}{D} \right)^{0.1} \right)} - 0.02 \right) \left(\frac{2c}{W - D} \right)^{N}$$

$$F_3 = 0.098 + 0.3592e^{-3.5089\frac{C}{R}} + 0.3817e^{-0.5515\frac{C}{R}}$$

For a = c = 0.10", R = 0.125", W = 2.70", D = 0.250", the above values are calculated to be F3 = 0.366, F_{ww} = 1.00, F_w = 1.01, $F_{c/R}$ = 1.44, β_1 = 1.45, β_2 = 0.55, β = 2.0 and the Stress Intensity K_I = 28ksi$\sqrt{in}$.

3 Plastic effects on Stress Intensity

If the idealized spar cross section is assumed to be made of 7075-T6510 Extrusion (L-T direction), then σ_{YS} = 67ksi, and it is determined whether plane stress or plane strain is to be used:

$$I = 6.7 - \frac{1.5}{t}\left(\frac{K_I}{\sigma_{YS}}\right)^2 = 6.7 - \frac{1.5}{0.50}\left(\frac{28}{67}\right)^2 = 6.18$$

This shows that the part is in plane strain (implying failure due to square fracture, consistent with purely Mode I – we will disregard mixed-mode analysis). Since I has been determined, this can be used to find the plastic zone size (r_p) and effective crack length (a_{eff}) to recalculate K_I. This is done through an iterative process:

$$r_p = \frac{1}{I\pi}\left(\frac{K_I}{\sigma_{YS}}\right)^2 \qquad K_I = \sigma\sqrt{\pi a_{eff}}\beta \qquad where\ a_{eff} = a + r_p$$

Therefore, with the plastic zone accounted for, K_I is calculated to be 29.3ksi$\sqrt{in}$ for an initial crack size of a = 0.1" (based on available inspection methods).

For a finite width plate with a center hole under remote uniaxial stress, the effect on increasing the initial crack size on K_I is shown in Fig 3.1. Note that this takes into account the plastic zone size as well.

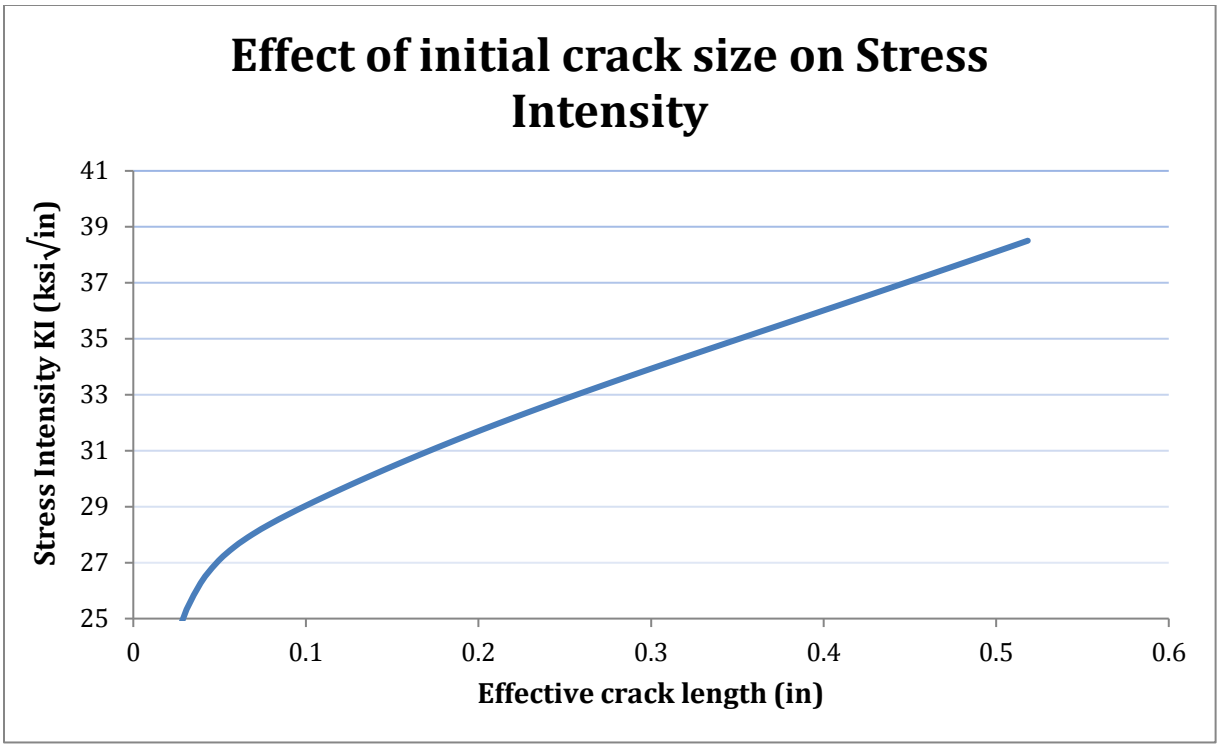

Figure 3.1: Effect of increasing Initial crack length on Stress Intensity

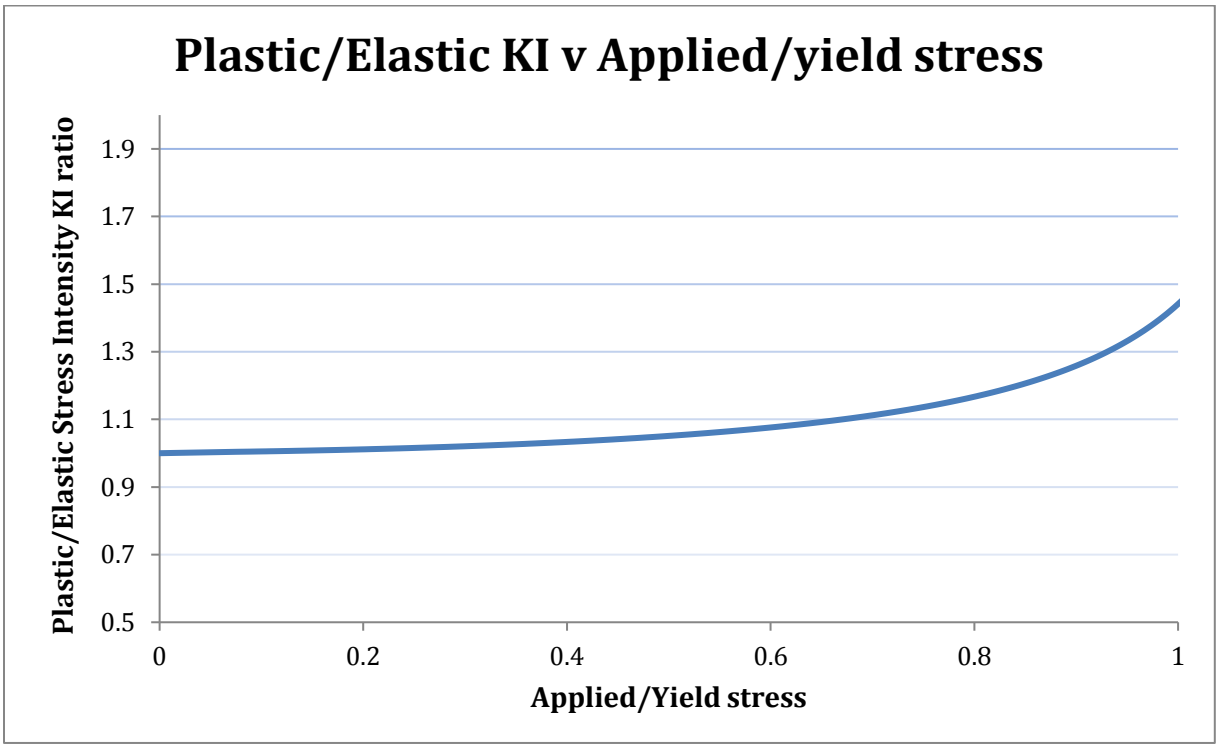

Figure 3.2: Ratio of Plastic/Elastic KI v Ratio of Applied Stress/Yield Stress

4 Residual Strength calculations

The values of residual strength for Net section yield and fracture toughness are plotted in Fig 4.1. The net section yield value for residual strength is calculated by:

$$\sigma_R = \sigma_{YS} \frac{A_{NET}}{A_{GROSS}}$$

The gross area is the cross sectional area of the part as seen in Fig 2.2 = (2.70 - 0.25)*0.5 = 1.225in2. The net area is calculated by varying the crack length and carrying out (2.70 – 0.250 – crack length)*0.50.

Additionally, the fracture toughness of the material is used to calculate the residual strength due to brittle fracture using:

$$\sigma_R = \sigma_C = \frac{K_C}{\sqrt{\pi a \beta}}$$

Using the chart on p115, 7050-T651 (closest material for data available) at Room Temp in the T-L direction, with a thickness of 0.50" has a Kc ≈ 43Ksi. This information is plotted in Fig 4.1 to construct a Residual Strength curve using the Federson method.

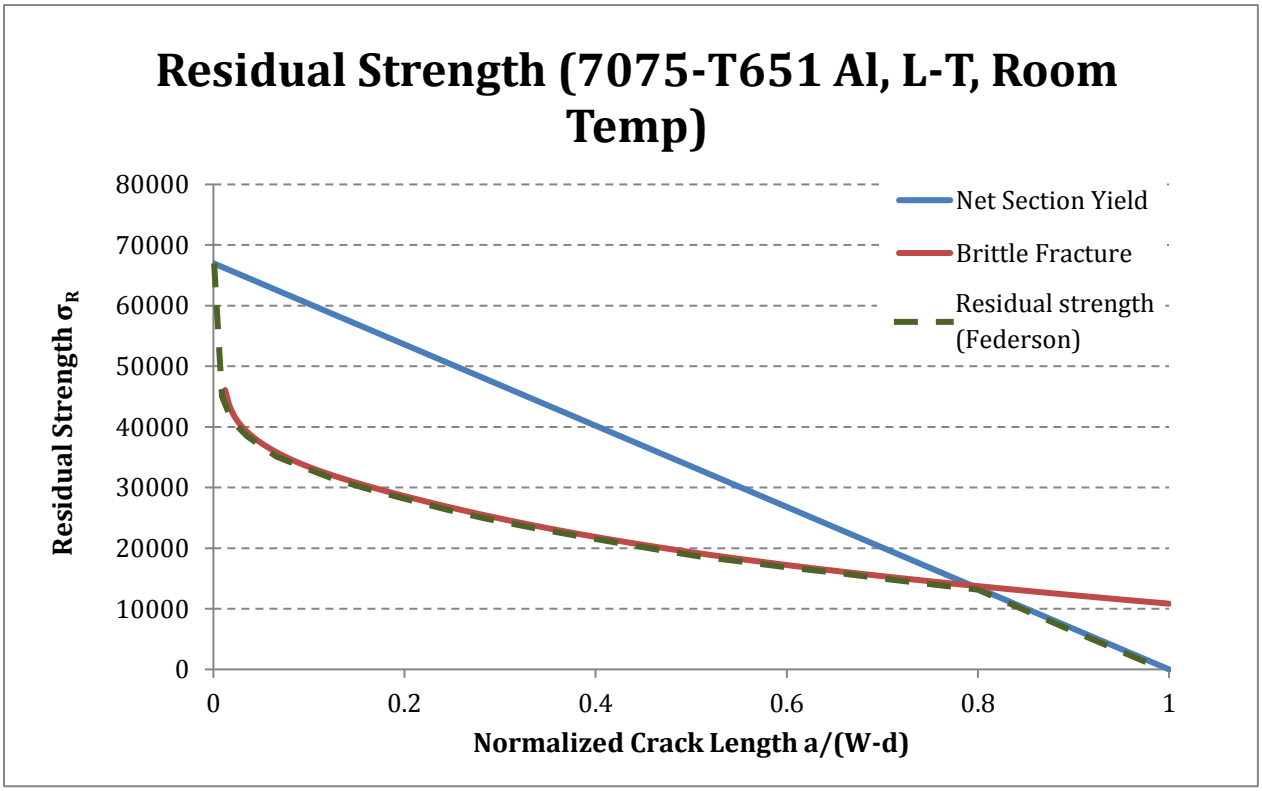

Figure 4.1: Residual Strength curve constructed using the Federson method (7075-T651 Al)

The graph above shows that for smaller crack lengths, failure at a range of stresses (~15ksi – 67ksi) occurs due to Brittle fracture rather than net section yield. It is only when the crack reaches a longer, more critical length, that the part fails due to net section yield. The same plot is constructed for 2 different materials at t=0.5", L-T, Room temperature: 2024-T3 Al (σ_{YS} = 44ksi, KC = 125ksi) and 15-5PH Steel (σ_{YS} = 160ksi, KC =160ksi) as seen in Fig 4.2 and Fig 4.3.

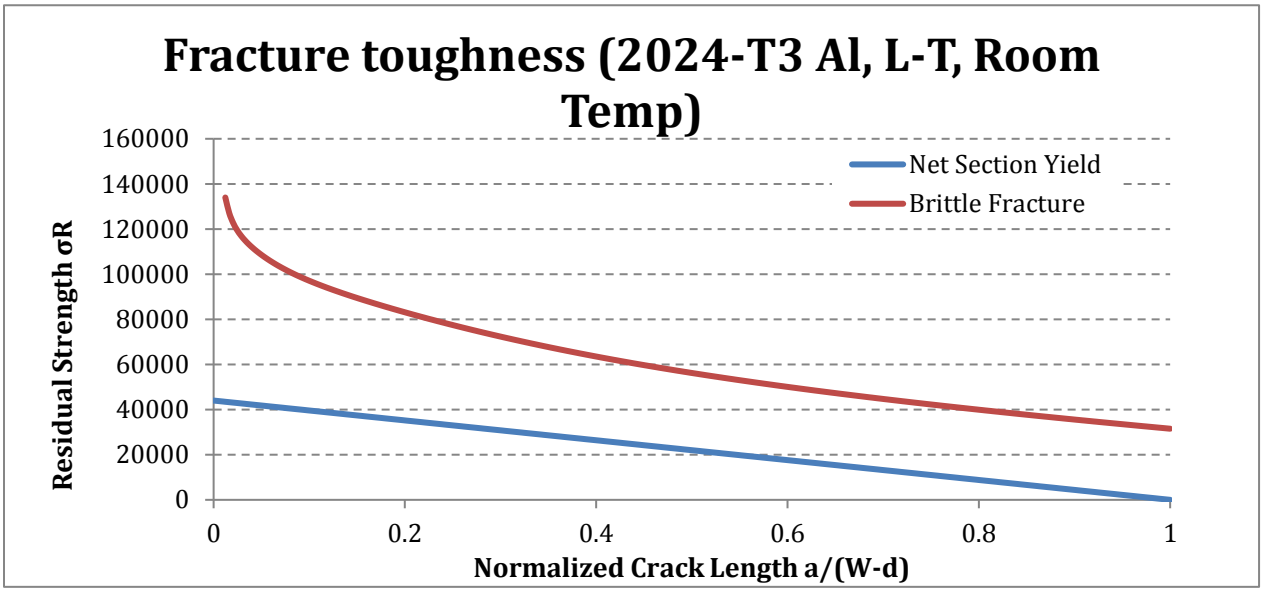

Figure 4.2: Residual Strength curve (2024-T3 Al)

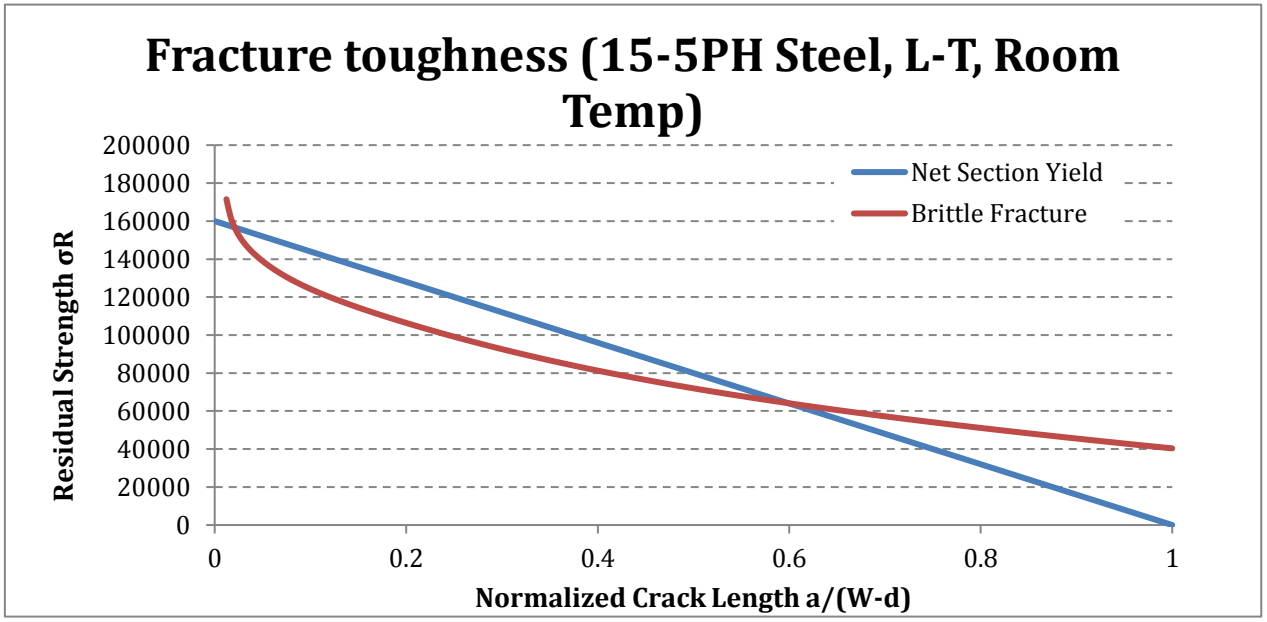

Figure 4.3: Residual Strength curve (15-5PH Steel)

For Fig 4.2, it is seen that the use of Al 2024-T3 causes failure through net section yield at both lower crack sizes as well as lower stresses. This material is less desirable to use in a part that undergoes cyclic loading with high stresses than the 7075-T651. This is compared to the Steel 15-5PH material, which does not predict failure until significantly high stresses (both through net section yield as well as brittle failure). However, it is important to note that the use of steel adds significant weight to the structure, and this is not suitable in an aerospace application.

5 Fatigue Life

Stress based fatigue

Stress based fatigue is used to analyze the structure at low stress, high cycles, where elastic effects are predominant and S-N curves of materials are used to predict cycles to failure.

Estimating the fatigue life of the spar is largely dependent on the spectrum of stresses experienced during the operation of the airplane. As mentioned in Section 1, the predominant loading case on the lower spar is tension due to wing up bending. This will be seen to occupy most of the spectrum, at different magnitudes. Additionally, the lower spar will also undergo compression during taxi, and landing conditions. This spectrum is visually presented in Fig 5.1.

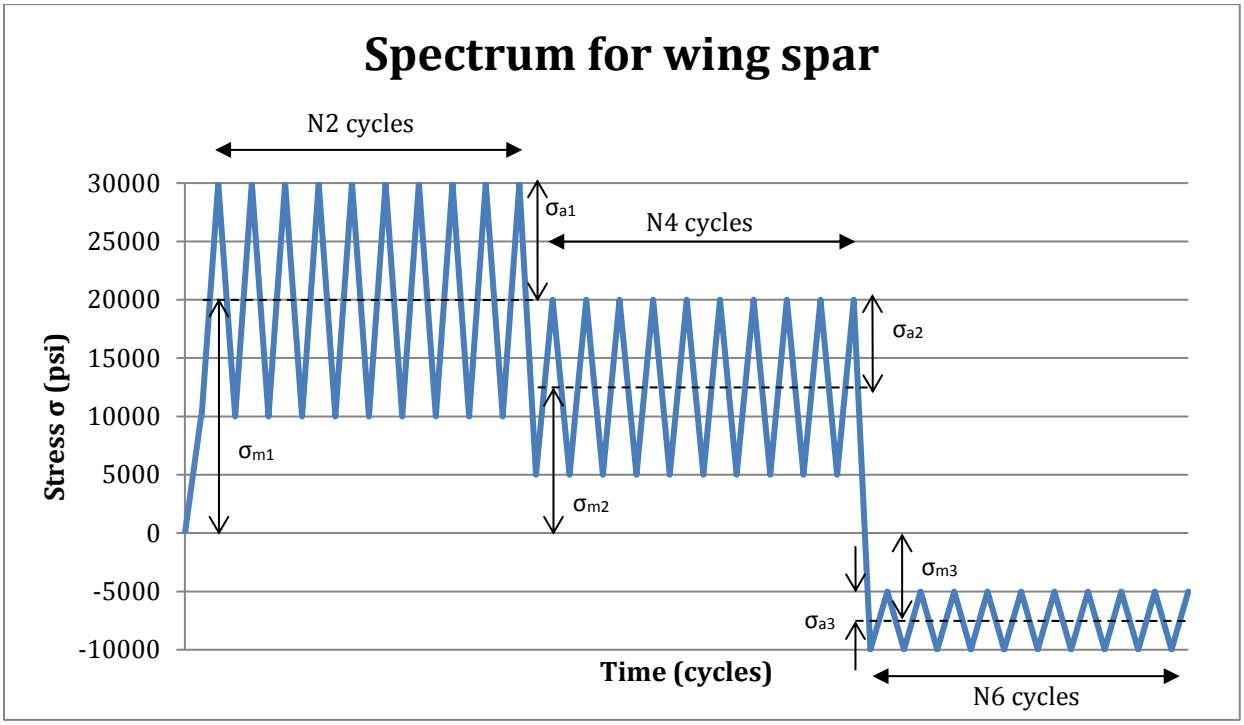

Figure 5.1: Flight spectrum for Spar

If the cycles above are counted, they can be represented in a table form:

j	Nj (# of cycles)	σ_{min} (Min Stress - psi)	σ_{max} (Max Stress - psi)	σ_a (Stress Amplitude – psi)	σ_m (Mean Stress – psi)	N_{fj}
1	0.5	0	10000	5000	5000	1.05E+11
2	9.5	10000	30000	10000	20000	4.89E+08
3	0.5	5000	30000	12500	17500	1.12E+08
4	9.5	5000	20000	7500	12500	4.77E+09
5	0.5	-10000	20000	15000	5000	4.84E+07
*6	9.5	-10000	-5000	2500	-7500	2.01E+13

*Note that the purely compressive stresses do not cause fatigue damage/crack growth, and are disregarded.

For the values in the above table, the values are calculated using:

$$\sigma_a = \frac{\sigma_{max} - \sigma_{min}}{2} \qquad \sigma_m = \frac{\sigma_{max} + \sigma_{min}}{2}$$

$$N_f = \frac{1}{2}\left(\frac{\sigma_a}{\sigma_f' - \sigma_m}\right)^{\frac{1}{b}}$$

Where σ'_f and b are material constants, and are defined for 7075-T651 as 213ksi and -0.143 respectively[1]. The equation above needs to be modified to take into account the non-zero mean stress for the various stress blocks using the Modified Goodman approach.

Using the spectrum above, the number of 'blocks' to failure is determined by the Palmgren-Miner rule:

$$B_f = \frac{1}{\left[\sum \frac{N_j}{N_{fj}}\right]} = \frac{1}{\frac{1}{1.05E+11} + \frac{1}{4.89E+08} + \cdots} = 3.14E+07\ repetitions$$

Strain based fatigue

In strain based fatigue, the strain amplitude is composed of elastic as well as plastic strain. The equations below take into account a mean stress σ_m also.

$$\varepsilon_a = \varepsilon_{ea} + \varepsilon_{pa} \qquad \varepsilon_{ea} = \frac{\sigma_{ar}}{E} = \frac{\sigma_f'}{E}\left(1 - \frac{\sigma_m}{\sigma_f'}\right)(2N_f)^b \qquad \varepsilon_{pa} = \varepsilon_f'(2N_f)^c$$

[1] http://www.ewp.rpi.edu/hartford/~ernesto/F2011/EP/MaterialsforStudents/Aiello/Dowling2004.pdf

Where ε_f' and c are material constants.

For 7075-T6 Al, ε_f' = 0.262, c = -0.619. We need to define a mean stress from a single cycle that is representative of the entire spectrum. A suitable means of doing this is to use the Boeing Commercial method to replace a single repeatable flight spectrum (as seen in Fig 5.1) with a single cycle where R = 0. Note that R is the Stress Ratio $\sigma_{min}/\sigma_{max}$.

c	Nj (# of cycles)	σ_{min} (Min Stress - ksi)	σ_{max} (Max Stress - ksi)	N_{fj}	R	z	N(1/z* σ_{max})^-P
1	0.5	0	10	1.05E+11	0.00	1.00	7.94E+03
2	9.5	10	30	4.89E+08	0.33	0.78	2.23E+05
3	0.5	5	30	1.12E+08	0.17	0.90	3.76E+05
4	9.5	5	20	4.77E+09	0.25	0.84	6.05E+04
5	0.5	-10	20	4.84E+07	-0.50	1.28	3.06E+05
						Sum	9.74E+05

Where $z = (1 - R)^q$, and p = 3.9, q = 0.6.

To find one equivalent stress:

$$\left(\frac{1}{S}\right)^{-p} = 9.74E + 05$$

$$S = (9.74E + 05)^{\frac{1}{3.9}} = 34.3Ksi$$

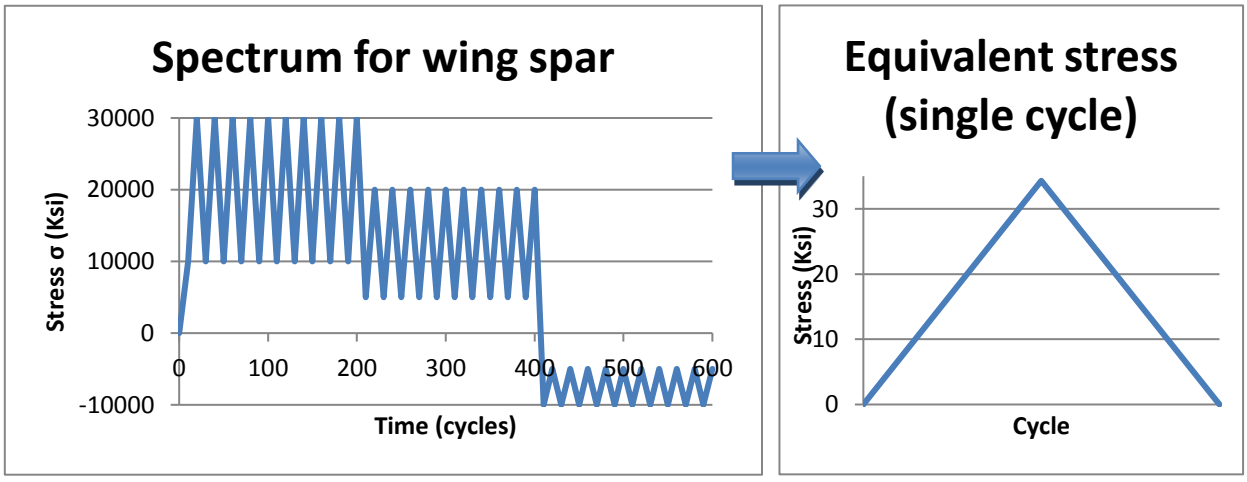

Figure 5.2: Flight spectrum for Spar, represented by a single cycle stress

Using the Smith Watson Topper approach, we calculate the elastic strain using the constants previously defined, as well as H' = 142, n' = 0.106, E = 10,300ksi. In this case, σ_a is the amplitude of the equivalent stress – 34.3/2 = 17.15ksi.

$$\varepsilon_a = \frac{\sigma_a}{E} + \left(\frac{\sigma_a}{H'}\right)^{\frac{1}{n'}} = \frac{17.15}{10300} + \left(\frac{17.15}{142}\right)^{\frac{1}{0.106}} = 0.000167$$

Using the relation $\sigma_{max}\varepsilon_a = \frac{(\sigma_f')^2}{E}(2N_f)^{2b} + \sigma_f'\varepsilon_f'(2N_f)^{b+c}$, and using σ_{max}=34.3ksi, numerical optimization is used to estimate the fatigue life at N_f=2.6 E10+06 cycles.

6 Crack growth

The rate of crack growth dA/dN can be calculated using a number of methods. In this analysis, the Paris law and the Boeing Walker method are compared to determine stable crack growth (Region II).

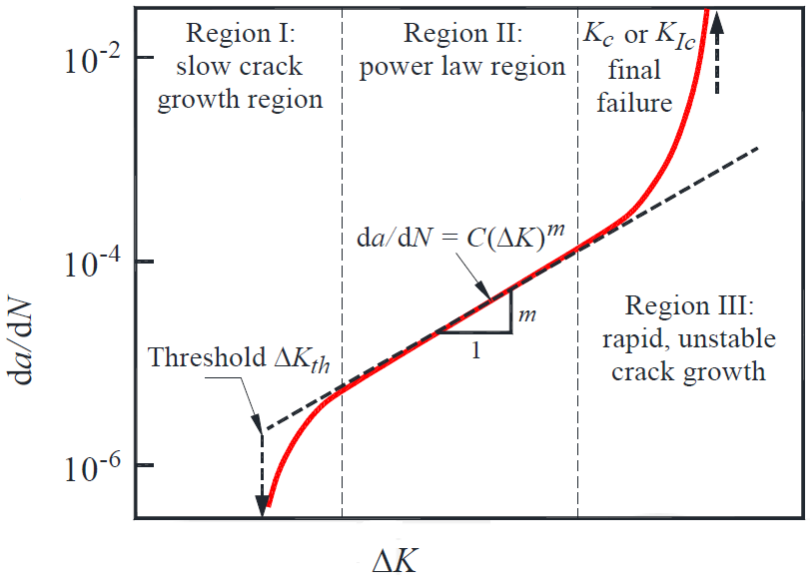

Figure 6.1: Regions of crack growth

Paris Law

The Paris law dictates that the crack growth depends on the following:

$$\frac{dA}{dN} = C(\Delta K)^n$$

Where C = 2.5 E10-9, n = 3.6[2] are material constants.

Walker-Boeing Method

The Walker-Boeing method calculates crack growth through:

$$\frac{dA}{dN} = \frac{10^{-4}(zK_{max})^p}{m_T^p}$$

Where $z = (1-R)^q$ for R≥0, and $z = (1-\mu R)$ for R≤0.

For 7075-T6511 Extrusion, p = 3.5, q = 0.6, μ = 0.1, MT = 22.6.

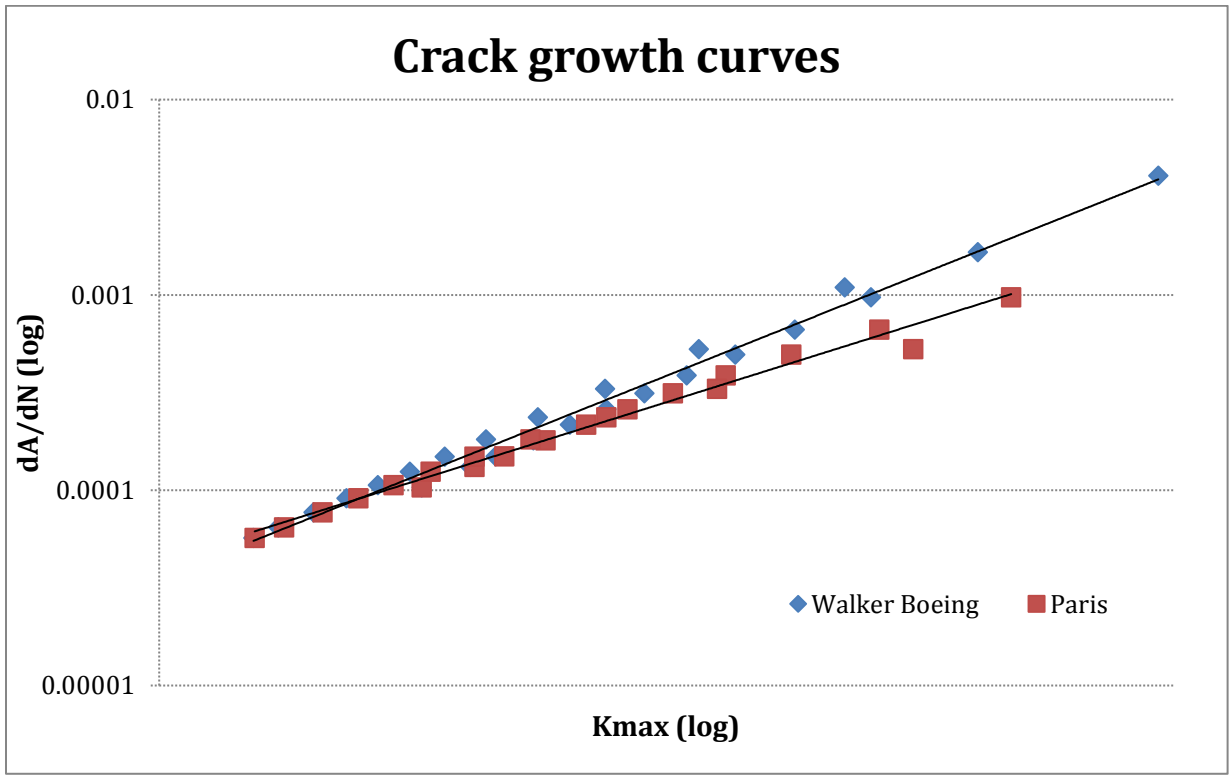

Figure 6.2: Crack growth rates (Boeing-Walker v Paris Law methods)

Using the Paris Law, dA/dN is integrated between the limits of the initial crack size (0.050") and the critical crack length (as calculated below) to determine the number of cycles to failure of the part. The spectrum is represented by a single max stress = 34.3ksi.

The critical length of the crack is calculated as follows:

[2] http://www.afgrow.net/applications/DTDHandbook/examples/page2_2.aspx

$$a_{crit} = \frac{1}{\pi}\left(\frac{K_C}{\beta\sigma_{max}}\right)^2 = \frac{1}{\pi}\left(\frac{125}{2.45 * 34.3}\right)^2 = 0.71\ inches$$

$$\frac{dA}{dN} = C(\Delta K)^n = C((1-R)K_{max})^n$$

$$\frac{dA}{dN} = C\left((1-R)\sigma_{max}\sqrt{\pi a}\beta\right)^n$$

$$\int_{a_0}^{a_{crit}} a^{\frac{-n}{2}}\, dA = \int_0^{N_f} C\left((1-R)\sigma_{max}\sqrt{\pi}\beta\right)^n\, dN$$

$$\left|-\frac{1}{a}\right|_{a_0}^{a_{crit}} = \left|NC\left((1-R)\sigma_{max}\sqrt{\pi}\beta\right)^n\right|_0^{N_f}$$

$$\left|-\frac{1}{a}\right|_{0.05}^{0.71} = N_f(2.5E-09) * \left((1-0.33)34.3\sqrt{\pi}2.45\right)^{3.6}$$

$$N_f \approx 544\ cycles$$

Using the above information, it is possible to set an inspection cycle to monitor crack growth in the part:

If the detectable crack length is set at 0.10", a detectable crack will appear at this location (using similar method as above) at approximately 290 cycles – this is a good point for an initial inspection. A recurring inspection can be set at 370 cycles and 460 cycles to detect any increases in crack length over the time interval.

7 Damage Tolerance Improvements

Some methods of improving damage tolerance for this part are:

- Improved manufacturing methods to guarantee smaller initial crack size

- Thinner flange of spar cap

- Added cross section at the location of the spar cap (through a strap, or similar) to reduce the maximum stress on the section

- More sophisticated NDI methods to detect smaller cracks

- 'Cold-working' the discrepant location, to introduce a residual compressive stress at the site, and to retard crack growth to an extent